Title
Assembly of the Light-Harvesting Chlorophyll Antenna in the Green Alga Chlamydomonas reinhardtii Requires Expression of the TLA2-CpFTSY Gene

Journal
Plant Physiology, 158(2)

ISSN
0032-0889

Authors
Kirst, Henning
García-Cerdán, Jose Gines
Zurbriggen, Andreas
et al.

Publication Date
2012-02-03

DOI
10.1104/pp.111.189910

Peer reviewed

Assembly of the Light-Harvesting Chlorophyll Antenna in the Green Alga *Chlamydomonas reinhardtii* Requires Expression of the *TLA2-CpFTSY* Gene[1][C][W][OA]

Henning Kirst, Jose Gines García-Cerdán, Andreas Zurbriggen, and Anastasios Melis*

Plant and Microbial Biology, University of California, Berkeley, California 94720–3102

The *truncated light-harvesting antenna2* (*tla2*) mutant of *Chlamydomonas reinhardtii* showed a lighter-green phenotype, had a lower chlorophyll (Chl) per-cell content, and higher Chl *a*/*b* ratio than corresponding wild-type strains. Physiological analyses revealed a higher intensity for the saturation of photosynthesis and greater P_{max} values in the *tla2* mutant than in the wild type. Biochemical analyses showed that the *tla2* strain was deficient in the Chl *a-b* light-harvesting complex, and had a Chl antenna size of the photosystems that was only about 65% of that in the wild type. Molecular and genetic analyses showed a single plasmid insertion in the *tla2* strain, causing a chromosomal DNA rearrangement and deletion/disruption of five nuclear genes. The *TLA2* gene, causing the *tla2* phenotype, was cloned by mapping the insertion site and upon complementation with each of the genes that were deleted. Successful complementation was achieved with the *C. reinhardtii TLA2-CpFTSY* gene, whose occurrence and function in green microalgae has not hitherto been investigated. Functional analysis showed that the nuclear-encoded and chloroplast-localized CrCpFTSY protein specifically operates in the assembly of the peripheral components of the Chl *a-b* light-harvesting antenna. In higher plants, a *cpftsy* null mutation inhibits assembly of both the light-harvesting complex and photosystem complexes, thus resulting in a seedling-lethal phenotype. The work shows that *cpftsy* deletion in green algae, but not in higher plants, can be employed to generate *tla* mutants. The latter exhibit improved solar energy conversion efficiency and photosynthetic productivity under mass culture and bright sunlight conditions.

Photosynthesis depends on the absorption of sunlight by chlorophyll (Chl) molecules in PSI and PSII. In higher plants and green algae, a completely functional but minimal PSI unit encompasses 95 Chl *a* molecules, while PSII functions with a minimal number of 37 Chl *a* molecules (Glick and Melis, 1988; Zouni et al., 2001). Increasing the number of light-harvesting pigments associated with each reaction center, upon the addition of peripheral Chl *a* and *b* molecules, is thought to afford a competitive advantage to the organism in an environment where sunlight is often limiting (Kirk, 1994). Photosynthetic organisms evolved a variety of such pigment-containing protein complexes associated peripherally with PSI and PSII. In higher plants and algae, these are referred to as Chl *a-b* light-harvesting complex (LHC)-I and LHC-II for photosystem-I (PSI) and photosystem-II (PSII) respectively. Photosystem-peripheral LHCs serve as auxiliary antennae for the collection of sunlight energy and as a conducting medium for excitation energy migration toward a photochemical reaction center (Smith et al., 1990). The Chl *a-b* LHCs increase the number of pigment molecules that are associated with the reaction centers, normally up to 250 for PSI and 300 for PSII (Ley and Mauzerall, 1982; Melis and Anderson, 1983; Smith et al., 1990; Melis, 1991).

The Chl antenna size of the photosystems is not fixed but is regulated by the level of irradiance seen by the photosynthetic apparatus (Smith et al., 1990; Melis, 1991; Ballottari et al., 2007). However, genes that direct a large size for the Chl antenna, and those that regulate the assembly of the LHCs are not well understood. In the model green algae *Chlamydomonas reinhardtii*, three genes are known to influence the accumulation of LHCs in the thylakoid membrane, namely *ALB3.1*, *TRUNCATED LIGHT-HARVESTING ANTENNA1* (*TLA1*), and *NAB1* (Bellafiore et al., 2002; Polle et al., 2003; Mussgnug et al., 2005; Tetali et al., 2007; Mitra and Melis, 2010). The nucleic acid binding protein NAB1 binds to the mRNA of the major *Lhcb* genes and thereby represses their translation (Mussgnug et al., 2005). Consequently, a deletion of the NAB1 gene derepresses *Lhcb* translation, leading to a larger Chl antenna size phenotype in NAB1-minus mutants. A mutant with a substantially down-regulated expression of the *TLA1* gene showed a lighter-green pheno-

[1] This work was supported by the U.S. Department of Energy, Hydrogen Program (grant no. DE–FG36–05GO15041), a Swiss National Science Foundation Postdoctoral Fellowship (grant no. PBBEP3_128360 to A.Z.), and a Swedish Research Council Postdoctoral Fellowship (grant no. 623–2010–586 to J.G.G.-C.).

* Corresponding author; e-mail melis@berkeley.edu.

The author responsible for distribution of materials integral to the findings presented in this article in accordance with the policy described in the Instructions for Authors (www.plantphysiol.org) is: Anastasios Melis (melis@berkeley.edu).

[C] Some figures in this article are displayed in color online but in black and white in the print edition.

[W] The online version of this article contains Web-only data.

[OA] Open Access articles can be viewed online without a subscription.

www.plantphysiol.org/cgi/doi/10.1104/pp.111.189910

type and a truncated light-harvesting Chl antenna size for both photosystems (Polle et al., 2003). TLA1 is highly conserved among eukaryotes and is thought to help define the size and number of organelles in the cell by an as-yet-unknown mechanism (Tetali et al., 2007; Mitra and Melis, 2010). The product of the *ALB3.1* gene, called ALB3 in higher plants, is a homolog of YidC of *Escherichia coli*, an inner membrane protein that facilitates incorporation of transmembrane proteins by the so-called signal recognition particle (SRP; Yi and Dalbey, 2005). In *C. reinhardtii*, ALB3.1 is nuclear encoded but targeted to the chloroplast. It is essential for the incorporation of the peripheral LHCs into the thylakoid membrane of photosynthesis (Bellafiore et al., 2002). The ALB3.1 protein is also known in Arabidopsis (*Arabidopsis thaliana*) but its function appears to extend beyond the transmembrane integration of LHCs, as it appears to also be needed for the assembly of PSI and PSII in the thylakoid membrane (Asakura et al., 2008).

The chloroplast SRP (CpSRP) is defined as a collection of four proteins that work together, including CpSRP54, CpSRP43, CpFTSY, and ALB3 (recent review, Aldridge et al., 2009). It is postulated that CpSRP54 and CpSRP43 operate in the chloroplast stroma, where they bind to hydrophobic domains of transmembrane proteins that are targeted for insertion into the thylakoid membrane and thereby keep them in solution. The receptor CpFTSY protein recognizes the CpSRP54-CpSRP43-target protein complex and guides the complex to the integral thylakoid membrane protein ALB3. The latter facilitates incorporation of the target protein into the thylakoid membrane. The CpSRP and its receptor protein CpFTSY are predicted to exist in green algae based on DNA sequence analysis but has not yet been experimentally verified. An Arabidopsis T-DNA knockout mutant of CpFTSY was missing most of the light-harvesting Chl proteins, but was also deficient in PSI and PSII core and reaction center proteins from the thylakoid membrane (Asakura et al., 2008). Furthermore, the *cpftsy* mutant in higher plants (e.g. Arabidopsis) was seedling lethal. A similar conclusion was reached for the *alb3* mutant of Arabidopsis (Asakura et al., 2008). The CpSRP component proteins in higher plants, namely CpSRP54 and CpSRP43, are postulated to be involved in the proper folding of light-harvesting proteins and targeting to the thylakoid membrane, thereby facilitating the biogenesis and assembly of the photosystem holocomplexes (Pilgrim et al., 1998; Amin et al., 1999; Klimyuk et al., 1999).

To better understand the genetic mechanism that defines the size of the light-harvesting antenna in green microalgae, and also in an effort to generate *TLA* mutants, we generated and screened a library of *C. reinhardtii* DNA insertional mutagenesis strains. This work presents a molecular, genetic, and physiological analysis of one of these mutants, termed *tla2*, which exhibited a stably truncated light-harvesting Chl antenna size. The corresponding *TLA2* gene was cloned and found to encode for a homolog of the SRP receptor CpFTSY protein. Detailed functional analysis revealed that the phenotype of the *tla2*-Δ*FTSY* mutant in *C. reinhardtii* differs from that in higher plants. Substantial reductions of the light-harvesting Chl antenna size in the *tla2*-Δ*FTSY* mutant are not accompanied by a lethal phenotype, which, in higher plants, is apparently due to inability to assemble both the LHC and the reaction centers of PSI and PSII. Unlike its higher plant counterparts, the *tla2*-Δ*CpFTSY* mutant assembles functional PSI and PSII reaction centers that support photoautotrophic growth of the cell. Accordingly, the *cpftsy* mutant phenotype and the CrCpFTSY gene can be employed in *C. reinhardtii* and possibly other green microalgae as a tool by which to truncate the Chl antenna size, without at the same time obliterating the function of the PSII and PSI reaction centers. Differences in the phenotype among plants and algae with a deleted *CpFTSY* gene are discussed.

RESULTS

Isolation of *C. reinhardtii* Strains with a Truncated Light-Harvesting Antenna Size (*tla* Mutants)

A library of over 15,000 transformant stains was generated via DNA insertional mutagenesis of *C. reinhardtii* strain CC-425 with linearized pJD67 plasmid (Davies et al., 1994). Exogenous DNA insertion into the genomic DNA of *C. reinhardtii* occurs randomly, occasionally interrupting nuclear-encoded genes, thus causing mutations. Transformant strains were initially isolated as Arg autotrophs, a property conferred upon transformation with pJD67 plasmid, as it contains a functional *ARG7* gene (Davies et al., 1996). Arg autotroph strains were screened as previously described (Polle et al., 2003), and also by measuring the Chl *a*/*b* ratio of colonies to identify putative *tla* mutants. Out of the initial 15,000 transformants, six strains displayed a substantially higher Chl *a*/*b* ratio than the corresponding parental wild type, indicating a putative smaller light-harvesting antenna size. One of these mutants, termed *tla2*, was selected for further analysis.

Characterization of the *tla2* Mutant: Pigment Content and Composition

Cells of the *tla2* strain, when cultivated as single-cell colonies on agar, displayed lighter-green coloration than their wild-type counterparts (Fig. 1). Biochemical analysis showed that, on a per-cell basis, the *tla2* strain accumulated only about 20% to 25% of the total Chl present in the wild type. It also showed an elevated Chl *a*/*b* ratio, suggesting lower amounts of the Chl *a*-*b* LHC in the mutant (Table I). The cellular content of Chl in wild type and *tla2* was measured upon growth under two different light conditions: low light (80 μmol photons m^{-2} s^{-1}) and medium light (450 μmol photons m^{-2} s^{-1}; Table I). Four wild-type strains were

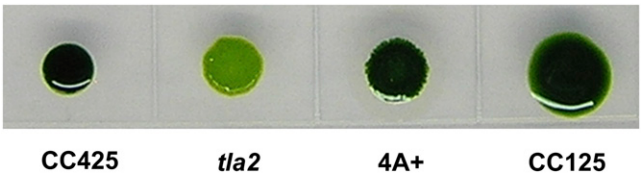

Figure 1. Single-cell colonies of *C. reinhardtii* wild type and *tla2* mutant grown on agar. Note the dark-green coloration of the wild-type strains, as compared to the light-green coloration of the *tla2* mutant. [See online article for color version of this figure.]

used as controls for this analysis. Strain CC-125 (*ARG7*, CW^+) is the parental wild-type strain of CC-425 (*arg2*, cw15). Strain 4A+ (*ARG7*, CW^+) was used for backcrosses with the *tla2* mutant. Strain CC-503 (*ARG7*, *cw92*) was also employed in this work, as this was applied by the U.S. Department of Energy Joint Genome Institute (JGI) to the *C. reinhardtii* genome sequencing (Merchant et al., 2007). All wild-type controls contained about 2.5 and 1.7 fmol Chl per cell when grown under low light and medium light, respectively, and had a Chl *a*/*b* ratio ranging between 2.7 and 3.0. A lower Chl/cell under medium-light growth conditions is a compensatory response of the photosynthetic apparatus to the level of irradiance, seeking to balance the light and carbon reaction of photosynthesis (Greene et al., 1988; Smith et al., 1990).

The *tla2* mutant displayed a substantially lower Chl content per cell under both irradiance-growth conditions, equal to about 20% of that in the corresponding wild-type controls: Under low-light growth, it was about 0.5 fmol Chl/cell and under medium light it was 0.3 fmol Chl/cell. The Chl *a*/*b* ratio in the *tla2* mutant was substantially greater than that of the wild type, and in the range of (8 to 10):1, reflecting absence of the auxiliary Chl *b* and possibly of a truncated light-harvesting Chl antenna size in this strain. The total carotenoid (Car) content in the *tla2* mutant was lower relative to that in the wild type, albeit not in proportion to that of Chl. Consequently, the Car/Chl ratio was about (0.4 to 0.5):1 in the wild-type strains and (0.8 to 0.9):1 in the *tla2* mutant.

Functional Properties and Chl Antenna Size Analysis of Wild Type and *tla2* Mutant

The functional properties of photosynthesis and the Chl antenna size of the *tla2* mutant were assessed from the light-saturation curve of photosynthesis, i.e. from the relationship between light intensity and photosynthetic activity measured under in vivo conditions (Melis et al., 1999; Polle et al., 2000, 2003). Light-saturation curves of photosynthesis were measured with wild type and *tla2* following cell acclimation to photoautotrophic growth at medium irradiance (growth at 450 μmol photons m^{-2} s^{-1}). At zero incident intensity (in the dark) the rate of oxygen evolution was negative (Fig. 2), reflecting oxygen consumption by the process of cellular respiration. Measured on a per-Chl basis, the rate of dark respiration of the *tla2* mutant was about 50% greater than that of the wild type (Fig. 2). This higher rate of respiration is partially due to the lower Chl content per cell in the mutant. However, rates of respiration on a per-cell basis were lower in the mutant, down to about 30% of those of the wild type (Table II).

In the light-intensity region of 0 to 400 μmol photons m^{-2} s^{-1}, the rate of photosynthesis increased as a linear function of light intensity, both in the wild type and *tla2* mutant (Fig. 2). These linear portions of the light-saturation curves were about parallel to one another, suggesting similar quantum yields of photo-

Table I. *Chl and Car content and pigment ratios for wild type, tla2 mutant, and tla2-complemented strains of C. reinhardtii (n = 3–5; means ± SD)*

Strain	Chl/Cell	Chl *a*/*b*	Car/Cell	Car/Chl
	fmol		*fmol*	
Low light (80 μmol photons m^{-2} s^{-1})				
4A+	2.57 ± 0.43	2.72 ± 0.07	1.07 ± 0.17	0.42 ± 0.00
CC-125	2.66 ± 0.13	3.00 ± 0.03	1.11 ± 0.06	0.42 ± 0.00
CC-504	2.36 ± 0.05	2.73 ± 0.05	0.93 ± 0.04	0.39 ± 0.01
CC-425	2.33 ± 0.10	2.86 ± 0.04	0.95 ± 0.04	0.41 ± 0.01
C1	1.93 ± 0.17	2.87 ± 0.02	0.67 ± 0.16	0.42 ± 0.00
C2	1.55 ± 0.04	3.01 ± 0.03	0.67 ± 0.00	0.43 ± 0.01
C3	1.06 ± 0.01	3.35 ± 0.16	0.54 ± 0.01	0.51 ± 0.00
C4	0.61 ± 0.09	3.92 ± 0.09	0.42 ± 0.05	0.68 ± 0.02
tla2	0.46 ± 0.04	9.60 ± 0.98	0.38 ± 0.00	0.82 ± 0.06
Medium light (450 μmol photons m^{-2} s^{-1})				
4A+	1.66 ± 0.37	2.45 ± 0.09	0.85 ± 0.17	0.51 ± 0.01
CC-125	1.85 ± 0.49	2.75 ± 0.14	1.01 ± 0.33	0.54 ± 0.04
CC-504	1.68 ± 0.33	3.08 ± 0.12	0.84 ± 0.13	0.50 ± 0.03
CC-425	1.35 ± 0.19	2.85 ± 0.04	0.74 ± 0.10	0.55 ± 0.01
C1	1.03 ± 0.04	2.71 ± 0.09	0.56 ± 0.03	0.54 ± 0.02
C2	0.71 ± 0.07	3.62 ± 0.11	0.52 ± 0.03	0.74 ± 0.03
C3	0.51 ± 0.07	4.36 ± 1.05	0.43 ± 0.07	0.85 ± 0.07
C4	0.35 ± 0.05	6.49 ± 0.56	0.34 ± 0.04	0.97 ± 0.02
tla2	0.33 ± 0.04	7.92 ± 0.83	0.30 ± 0.03	0.90 ± 0.01

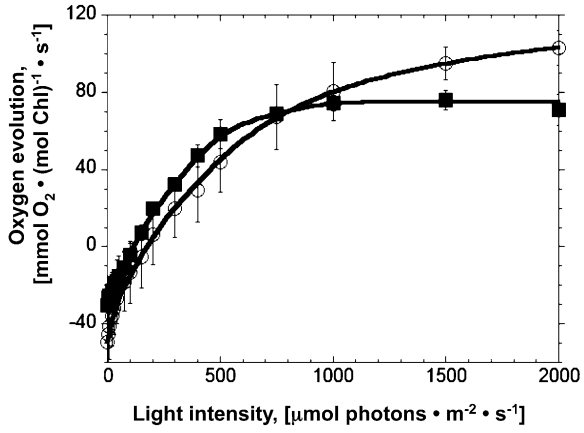

Figure 2. Light-saturation curves of photosynthesis obtained with the *C. reinhardtii* wild type (black squares) and the *tla2* mutant (white circles). The initial slopes of both curves are similar, suggesting equal quantum yield of the photosynthesis. The light-saturated rate P_{max} was greater in the *tla2* mutant than in the wild type, suggesting a greater productivity on a per-Chl basis in the *tla2* than in the wild type.

synthesis for the two strains. This is an important consideration, as it shows that the *tla2* mutation did not interfere with the high innate quantum yield of photosynthesis. The rate of photosynthesis in the wild type saturated at about 500 μmol photons m^{-2} s^{-1} (Fig. 2, black circles), whereas that of the mutant continued to increase with light intensity through the 2,000 μmol photons m^{-2} s^{-1} level. From the average of several measurements, the light-saturated rate (P_{max}) for the wild type was about 75 mmol O_2 (mol Chl)$^{-1}$ s^{-1}, whereas P_{max} for the *tla2* mutant was about 105 mmol O_2 (mol Chl)$^{-1}$ s^{-1}.

The light-saturated rate of photosynthesis is a measure of the overall photosynthetic capacity (P_{max}; Powles and Critchley, 1980). A large wild-type light-harvesting Chl antenna causes saturation of photosynthesis at about 500 μmol photons m^{-2} s^{-1} (Fig. 2). A much higher light intensity of bright sunlight, >2,000 μmol photons m^{-2} s^{-1}, was needed to saturate photosynthesis in the *tla2* mutant. Important in the context of this work is the light intensity required to bring about the rate of photosynthesis to the half-saturation point. The half-saturation intensity for the wild type was measured to be about 210 μmol photons m^{-2} s^{-1}, while for the *tla2* mutant it was 380 μmol photons m^{-2} s^{-1}. Since there is a reciprocal relationship between the half-saturation intensity of photosynthesis and the Chl antenna size, it may be concluded that photosystems (PSII and PSI) in the *tla2* mutant collectively possess only about 55% the Chl antenna size found in the corresponding wild type. Such differences in the half-saturation intensity and P_{max} are typical among fully pigmented and truncated Chl antenna microalgae (Melis et al., 1999; Polle et al., 2000, 2003).

A more precise determination of the functional Chl antenna size of PSI and PSII units in wild type and the *tla2* mutant was conducted by the spectrophotometric and kinetic method developed in this lab (Melis, 1989). The number of Chl molecules associated with each photosystem is given in Table II, measured in photoautotrophically grown cells under 450 μmol photons m^{-2} s^{-1}. The number of Chl molecules of $PSII_\alpha$ and $PSII_\beta$ was determined to be 250 and 90 for the wild type, respectively. These numbers were lowered to 160 and 90 for the *tla2* mutant. The proportional abundance of $PSII_\alpha$ and $PSII_\beta$ changed as a result of the mutation from 60:40 ($PSII_\alpha$:$PSII_\beta$) in the wild type to 45:55 in the mutant. Thus, an average of 190 Chl molecules is associated with the reaction centers of PSII in the wild type, while the average PSII antenna size of the *tla2* mutant was lowered to 120 Chl molecules (63%). The number of Chl molecules associated with a PSI reaction center was determined to be 210 for the wild type and 120 for the *tla2* mutant. Thus, the PSI antenna size of the *tla2* mutant was only about 60% of that in the wild type.

Table II. *Photosynthesis, respiration, and photochemical apparatus characteristics of wild type and the tla2 mutant of C. reinhardtii grown photoautotrophically under medium-light (450 μmol photons m^{-2} s^{-1}) conditions*

Photosystem Chl antenna size and reaction center concentrations were measured spectrophotometrically (Melis, 1989). WT, Wild type; $n = 3$; means ± SD.

Parameter Measured	WT	*tla2*
Respiration (mmol O_2 [mol Chl]$^{-1}$ s^{-1})	30.2 ± 11.9	49.1 ± 15.2
Respiration (amol O_2 cell^{-1} s^{-1})	55.8 ± 26.3	16.2 ± 5.4
Quantum yield, relative units	100 ± 25	108 ± 17
Photosynthesis (mmol O_2 [mol Chl]$^{-1}$ s^{-1})	106.3 ± 12.8	152.3 ± 18.0
Photosynthesis (amol O_2 cell^{-1} s^{-1})	196.2 ± 46.2	50.3 ± 7.3
Photosynthesis/respiration capacity ratio	3.5 ± 1.9	3.1 ± 1.1
Half-saturation intensity (μmol photons m^{-2} s^{-1})	210	380
Functional PSIIα Chl antenna size	249 ± 27	160 ± 7
Functional PSIIβ Chl antenna size	90 ± 30	90 ± 12
Fraction of PSIIα (%)	61 ± 1	46 ± 1
Average PSII Chl antenna size	190 ± 20	120 ± 9
Functional PSI Chl antenna size	180 ± 9	123 ± 5

To investigate if the loss of photosystems and light-harvesting antenna affects photoautotrophic growth, we measured the doubling time of *tla2* in comparison with the wild type under medium-light (450 μmol photons m^{-2} s^{-1}) conditions. The doubling time of the wild type at this light intensity was determined to be 6.3 ± 0.1 h, whereas the *tla2* mutant doubled every about 7.2 ± 0.3 h. This difference is consistent with the difference in the rate of oxygen evolution between the two strains at 450 μmol photons m^{-2} s^{-1} (Fig. 2).

The above functional and antenna analysis provided a foundation upon which the *tla2* strain was deemed to be a good candidate for the identification of gene(s) impacting the Chl antenna size of the photosystems. Accordingly, a detailed molecular and genetic analysis was undertaken to map the plasmid insertion site and to test for plasmid and lesion cosegregation in the *tla2* mutant, prior to gene cloning.

Insert-Site Genomic DNA Structure in *tla2* Mutant and Wild Type

Southern-blot analyses were used to determine the number of pJD67 plasmid insertions and their integrity in the genomic DNA of the *tla2* strain. Detailed descriptions of the Southern-blot analyses for the wild type and *tla2* mutant (Supplemental Fig. S1), as well as mapping of the pJD67 insertion site in the *tla2* genomic DNA (Supplemental Fig. S2) are provided in Supplemental Text S1. The analysis revealed a single pJD67 plasmid insertion in the *tla2* mutant. The locus of insertion was determined by Thermal Asymmetric InterLaced-PCR (TAIL-PCR) to be on chromosome number 5 in the coding sequence of predicted gene Cre05.g239000. Further investigation by Southern blot and genomic DNA sequencing analysis revealed unusual and major chromosomal DNA rearrangements in the *tla2* mutant. These included deletion of a 12.5-kb segment of the genomic DNA in the site of insertion, comprising three genes, namely Cre05.g241450, Cre05.g241500, and Cre05.g241550 (Fig. 3). In addition, a 358-kb segment of the genomic DNA flipped by 180° in orientation (5′ to 3′) in the *tla2* mutant, disrupting the continuity of two additional genes at each end of the rearrangement site, namely Cre05.g239000 and Cre05.g241400 (Fig. 3). Thus a total of five genes were affected by the pJD67 insertion in the *tla2* mutant. A simplified schematic of the insert-site genomic DNA structure in the *tla2* mutant and wild type is given in Figure 3, depicting the five putative genes that were affected.

Point of pJD67 Insertion Is Linked with the *tla2* Phenotype

Genetic crosses were used to test if the point of pJD67 insertion is directly responsible for the *tla2* phenotype. This is an important consideration, as the *tla2* lesion could have occurred inadvertently in a locus distinct and far away from the pJD67 insertion site. To eliminate background mutations that do not contribute to the phenotype of *tla2*, progeny of the fourth cross of the original *tla2* strain with Arg-requiring strain AG1-3.24 (*arg2*) were used in the below genetic crosses and PCR analysis.

Ten complete tetrads were plated on nonselective media containing Arg (Tris-acetate-phosphate [TAP] + ARG) and on plates selective for the presence of a functional *ARG7* gene within the insertion (TAP only). Figure 4 shows one typical tetrad analysis from such genetic crosses (a total of 10 tetrads were analyzed). When daughter cells were grown on TAP + ARG plates, the tetrad included two viable dark-green and two viable pale-green colonies (Fig. 4, top section). The dark-green daughter cell colonies had a wild-type Chl *a*/*b* ratio (Chl *a*/*b* = approximately 2.7:1). A high Chl *a*/*b* ratio (approximately 9:1) was measured for the pale-green daughter cell colonies. A 2:2 wild type to

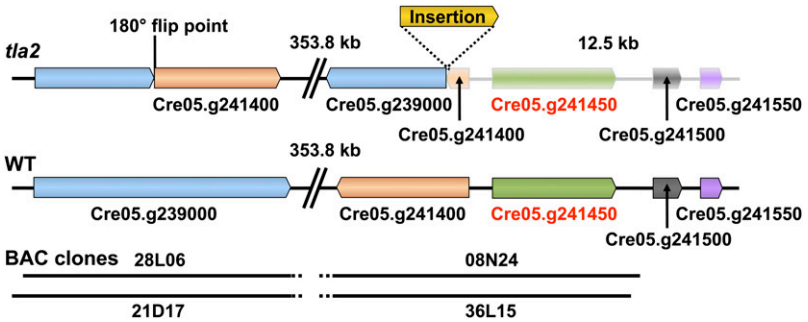

Figure 3. Map of the *tla2* and wild-type *C. reinhardtii* genomic DNA in the pJD67 insertion site. Plasmid insertion in the *tla2* mutant caused deletion of a 12.5-kb segment comprising three genes, namely Cre05.g241450, Cre05.g241500, and Cre05.g241550. In addition, a 358-kb segment of the *tla2* genomic DNA flipped by 180° in orientation (5′ to 3′), disrupting the continuity of two additional genes at each end of the rearrangement site, namely Cre05.g239000 and Cre05.g241400. Thus a total of five genes were affected by the pJD67 insertion in the *tla2* mutant. Also shown is the *C. reinhardtii* genomic DNA region covered in BAC clones 28L06, 21D17, 08N24, and 36L15. The plasmid insertion site and the identity of the *TLA2* gene (Cre05.g241450 in red font) are also indicated. [See online article for color version of this figure.]

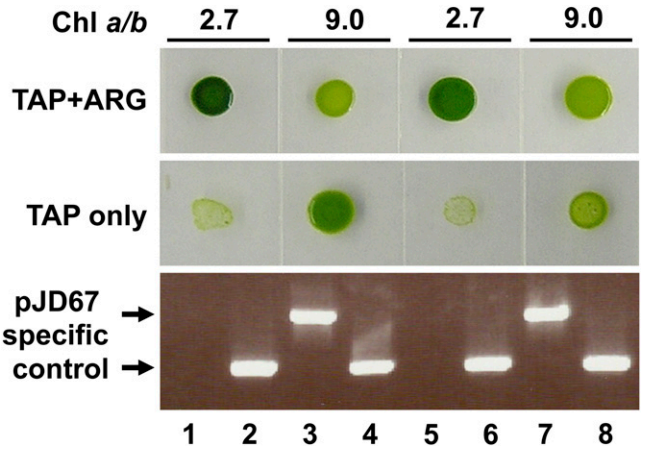

Figure 4. Genetic cross analysis of *tla2* with AG1x3.24 (*arg2*) strain. One representative tetrad from a single cross is shown (a total of 10 tetrads were analyzed), plated on nonselective TAP + ARG media (top section), or selective TAP-only media (middle section). The Chl *a*/*b* ratio of these progeny is shown at the top of the sections. The bottom section shows the result of PCR reactions, two lanes per progeny: The PCR reaction using an insertion-specific primer set was loaded on lanes 1, 3, 5, 7, and a positive control PCR on lanes 2, 4, 6, and 8. [See online article for color version of this figure.]

tla2 phenotype segregation was found among the progeny of all tetrads that were tested, providing strong evidence that a single genetic locus is causing the *tla2* phenotype. When plated on TAP-only agar plates (absence of Arg), the dark-green daughter cells could not grow, apparently because they lacked a functional *ARG7* gene and, therefore, lack Arg autotrophy (Fig. 4, middle section). Cells able to grow on selective media were exclusively pale-green progeny, suggesting a linkage between the *tla2* phenotype and the inserted pJD67 plasmid.

To further test whether the insertion locus is cosegregating with the *tla2* phenotype, we used genomic DNA PCR analysis. A forward primer in predicted Cre05.g239000 open reading frame and a reverse primer in the pJD67 sequence were employed. This combination of primers would generate a product only in the daughter cells of a genetic cross that actually carried the pJD67 insertion. As a positive control, a set of primers was used from a genomic DNA region of *C. reinhardtii* not affected by the insertion. Figure 4 (bottom section) shows that dark-green daughter cells failed to generate a pJD67-specific product (lanes 1 and 5) whereas they generated a product from the control primers (lanes 2 and 6). Pale-green daughter cells, on the other hand, generated both an insertion-specific (lanes 3 and 7) and a control-specific product (lanes 4 and 8). These findings were observed with all tetrads examined. In conclusion, results of the PCR analysis are consistent with the genetic analysis and strongly suggest that a single locus is causing the *tla2* phenotype and, furthermore, that it is linked with the pJD67 insertion site.

Cloning of the *TLA2* Gene

Using information from the sequenced *C. reinhardtii* genome and the bacterial artificial chromosome (BAC)-end DNA we searched for BAC clones comprising the five deleted genes in the *tla2* mutant. Two BAC clones, namely 28L06 and 21D17, were identified and shown to contain Cre05.g239000. Two other BAC clones, namely 08N24 and 36L15 were identified and shown to contain the genes Cre05.g241400 and Cre05.g241450. We could not find a BAC clone that comprises genes Cre05.g241500 and Cre05.g241550. Each of the four identified BAC clones were used along with pBC1 (conferring paromomycin resistance) in a cotransformation approach to complement the *tla2* strain. Transformants that grew on a paromomycin plate were screened for strains with a complemented *tla2* phenotype. This was done upon measurement of the Chl/cell and the Chl *a*/*b* ratio of the transformant colonies. Transformation with BAC clones 28L06 and 21D17 failed to generate any complemented strains. However, BAC clones 08N24 and 36L15 (Fig. 3) both successfully complemented the *tla2* phenotype in about 50% of the cotransformed algae. The latter showed a dark-green coloration and a low Chl *a*/*b* ratio phenotype. BAC clones 08N24 and 36L15 contain two predicted *C. reinhardtii* genes, Cre05.g241400 and Cre05.g241450. These two genes were tested separately, as cDNA constructs, for their ability to complement the *tla2* phenotype. For this purpose, the corresponding start and stop codon of the full-length mRNA of both genes was identified by 5′ and 3′ RACE. Both cDNAs were then cloned separately into pSL18 (conferring paromomycin resistance) for transformation of the *tla2* mutant. Transformation with Cre05.g241400 cDNA did not yield any complemented strains, while the cDNA construct of gene Cre05.g241450 yielded complements in which the wild-type phenotype was recovered to various degrees. These results suggested that deletion of gene Cre05.g241450 is responsible for the *tla2* phenotype. Gene Cre05.g241450 is predicted to encode a putative FTSY precursor protein with a chloroplast-targeted transit peptide. A putative CpFTSY protein has not been previously reported or characterized in *C. reinhardtii*, to our knowledge.

The *CpFTSY* gene of *C. reinhardtii* is 6,578-bp long and consists of 13 exons and 12 introns. The *CpFTSY* mRNA is 1,814 bp in length with a 5′ and 3′ untranslated region of 189 and 479 bp, respectively. The gene encodes for a protein of 381 amino acids including a putative 36 amino acid chloroplast-targeting sequence as determined by ChloroP (http://www.cbs.dtu.dk/services/ChloroP/) and TargetP (http://www.cbs.dtu.dk/services/TargetP/) software (Fig. 5). The mature protein of 345 amino acids with a M_r of 38.2 kD shares significant sequence homology with the SRP54 N-terminal helical bundle domain (amino acids 33–105) and the SRP54-type GTPase domain (amino acids 126–333) as determined from the database of Protein Families (Pfam)

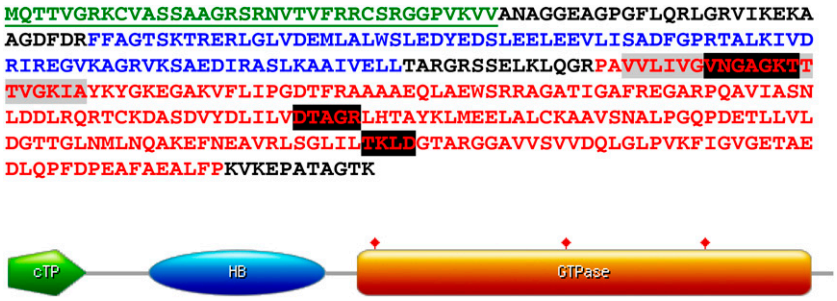

Figure 5. Top, Amino acid sequence of the *C. reinhardtii* FTSY protein. Domains of the CrCpFtsY protein are defined as follows: amino acids 1 to 36, transit peptide (green font). Amino acids 66 to 147, helical bundle domain (Pfam), SRP54-type protein (blue font). Amino acids 162 to 370, GTPase domain (Pfam), SRP54-type protein (red font). Amino acids 164 to 183, P-loop nucleotide binding motif, (pre; red, gray-shaded font). Amino acids 170 to 176, 258 to 262, and 322 to 325, homologous nucleotide binding (red, black-background font). Bottom, Domain presentation of the CrCpFTSY protein. CpTP, Chloroplast transit peptide; HB, helical bundle domain; GTPase, GTPase domain. [See online article for color version of this figure.]

(http://pfam.sanger.ac.uk; Fig. 5). These domains are universally conserved in SRP receptor proteins (Luirink and Sinning, 2004), suggesting that Cre05.g241450 encodes for the CpFTSY protein in the model green alga *C. reinhardtii.*

Homology of the Putative CrCpFTSY with Other CpFTSY Proteins

A ClustalW analysis and comparison of the putative CrCpFTSY with the known CpFTSY proteins of Arabidopsis (GenBank accession no. NP_566056) and maize (*Zea mays*; GenBank accession no. NP_001105732) was undertaken (Fig. 6). The comparative amino acid sequence analysis showed 46.1% identity and 61.9% similarity of the CrCpFTSY to AtCpFTSY and 50.5% identity and 65.5% similarity to ZmCpFTSY. Furthermore, a ClustalW amino acid sequence analysis of the putative CrCpFTSY identified in this work with the *C. reinhardtii* cytoplasmic SRα subunit homolog of the signal recognition receptor (GenBank accession no. XP_001692081) showed dissimilarity between these proteins, both in terms of amino acid sequence alignment and in terms of length between the two polypeptides (Supplemental Fig. S3). This bioinformatic analysis strengthened the notion of a chloroplast local-

Figure 6. CLUSTAL 2.1 multiple sequence alignment of AtCpFTSY, ZmCpFTSY, and CrCpFTSY. The comparative amino acid sequence analysis showed 46.1% identity and 61.9% similarity of the CrCpFTSY to AtCpFTSY and 50.5% identity and 65.5% similarity to ZmCpFTSY, strengthening the notion of a chloroplast localization and function for the CrCpFTSY identified in this work.

```
AtCpFTSY    MATSSAHLSFLAGRISPFSSERIGLFPLRGEFRPRMTRFRCSAG---PSGFFTRLGRLIK 57
ZmCpFTSY    MAAPSHVLPFLS----PAGGCAASSARAHSGYRAGLLRCSAAAG---QAGFFTRLGRLIK 53
CrCpFTSY    MQTTVGRKCVAS----SAAGRSRNVTVFRRCSRGGPVKVVANAGGEAGPGFLQRLGRVIK 56
            * :.     . :    . ..   .    :   *    :  . **    .**: ****:**

AtCpFTSY    EKAKSDVEKVFSGFSKTRENLAVIDELLLFWNLAETDRVLDELEEALLVSDFGPKITVRI 117
ZmCpFTSY    EKAKSDVEKLFSGFSKTRENLSVVDELLTYWNLADTDRVLDDLEEALLVSDFGPKISFRI 113
CrCpFTSY    EKAAGDFDRFFAGTSKTRERLGLVDEMLALWSLEDYEDSLEELEEVLISADFGPRTALKI 116
             *** .*.::.*:* *****.*.::**:*  *.* : :  *::***.*: :****: :.:*

AtCpFTSY    VERLREDIMSGKLKSGSEIKDALKESVLEMLAKKNSKTELQLGFRKPAVIMIVGVNGGGK 177
ZmCpFTSY    VDTLREEIRDGKLKSGAEIKAALKRCILELLTSKGGNSELNLGFRKPAVIMIVGVNGGGK 173
CrCpFTSY    VDRIREGVKAGRVKSAEDIRASLKAAIVELLTARGRSSELKLQGR-PAVVLIVGVNGAGK 175
            *: :** :  *::**. :*: :** .::*:*: :. .:**:*  * ***::******.**

AtCpFTSY    TTSLGKLAHRLKNEGTKVLMAAGDTFRAAASDQLEIWAERTGCEIVVAEGDKAKAATVLS 237
ZmCpFTSY    TTSLGKLAYRFKNEGVKVLMAAGDTFRAAARDQLEVWAERTGSEIVIDNDKKAQPPAVLS 233
CrCpFTSY    TTTVGKIAYKYGKEGAKVFLIPGDTFRAAAAEQLAEWSRRAGATIGAFREGARPQAVIAS 235
            **::**:*::  :**.**:: .******** :**  *:.*:*. *   .      ..: *

AtCpFTSY    ------KAVKRGKEEGYDVVLCDTSGRLHTNYSLMEELIACKKAVGKIVSGAPNEILLVL 291
ZmCpFTSY    ------QAVKRGKREGFDVVLCDTSGRLHTNYGLMEELVSCKKVLAKALPGAPNEILLVL 287
CrCpFTSY    NLDDLRQRTCKDASDVYDLILVDTAGRLHTAYKLMEELALCKAAVSNALPGQPDETLLVL 295
                  : . :.  : :*::* **:***** * *****  ** .::.: :.* *:* ****

AtCpFTSY    DGNTGLNMLPQAREFNEVVGITGLILTKLDGSARGGCVVSVVEELGIPVKFIGVGEAVED 351
ZmCpFTSY    DGTTGLNMLQQAREFNDVVGVTGFILTKLDGTARGGCVVSVVDELGIPVKFIGVGEGMED 347
CrCpFTSY    DGTTGLNMLNQAKEFNEAVRLSGLILTKLDGTARGGAVVSVVDQLGLPVKFIGVGETAED 355
            **.****** **:***:.* ::*:*******:****.*****::**:*********  **

AtCpFTSY    LQPFDPEAFVNAIFS----------- 366
ZmCpFTSY    LQPFDAEAFVEAIFP----------- 362
CrCpFTSY    LQPFDPEAFAEALFPKVKEPATAGTK 381
            *****.***.:*:*.
```

ization and function for the CrCpFTSY identified in this work.

Complementation of the *tla2* Strain with the CpFTSY cDNA

Complementation of the *tla2* strain with a wild-type *CrCpFTSY* cDNA resulted in the isolation of several transformant lines, which showed various degrees of wild-type recovery in their phenotype. The phenotypic complementation ranged anywhere between that of wild type and *tla2* mutant. Some successfully transformed lines failed to rescue the mutation altogether. This variable effectiveness of the *tla2* complementation is attributed to cDNA insertions in different regions of the chromosomal DNA in *Chlamydomonas*, many of which are either slow transcription zones, or are subject to epigenetic silencing. Four *tla2*-complemented lines were chosen for further detailed characterization, namely C1, C2, C3, and C4. Of those, C1 had a phenotype closest to the wild type, both in terms of the Chl/cell and Chl *a*/*b* ratio (Table I). It was the best-complemented line out of the four lines investigated. It had a Chl *a*/*b* ratio of 2.7 to 2.9 under either low- or medium-light conditions, which is in the same range as that of the wild type. The Chl/cell content of C1 was slightly lower under low light compared to the wild-type strains with about 1.9 fmol Chl per cell. Under medium light this difference was exacerbated, with C1 cells containing about 1.0 fmol Chl, i.e. only about 60% of that in the wild type. However, under both low-light and medium-light growth conditions the Chl/cell in C1 was substantially greater than that in the *tla2* mutant. C2, C3, and C4 lines were shown to be partially complemented strains of the *tla2* mutant, with C2 having the highest and C4 the lowest Chl/cell, while the numbers for C3 were found to be in between those of C2 and C4. This gradient of complementation from C1 to C4 was true for all photochemical apparatus parameters measured (Table I).

To further characterize the phenotype of the *tla2* mutation in relation to wild type, western-blot analyses with specific PSII and LHC-II antibodies were undertaken (Fig. 7) using cells grown photoautotrophically under medium light. Lanes were loaded on an equal cell basis, except for the wild type, where dilutions of 25% (about equal reaction centers) and 12% cells were loaded. All LHC-II proteins were either substantially lowered or not detected in the *tla2* mutant. Proteins cross-reacting with the Lhcb1-specific and Lhcb2-specific antibodies were lowered the most in abundance, down to about 10% of wild-type levels, while Lhcb3 was not detectable in the *tla2* mutant. The minor antenna protein, cross-reacting with Lhcb4-specific antibodies, was reduced to less than 5% of the wild-type levels and no cross-reaction could be detected using an antibody raised against the Lhcb5 protein. The PSII reaction center protein D2 also showed a lower abundance on a per-cell basis, down to about 20% to 25% of the wild type. However, loss of the peripheral Chl *a*-*b* antenna binding proteins is proportionally higher than the lowering of the photosystem reaction center proteins, consistent with the notion of a truncated light-harvesting antenna phenotype in the *tla2* mutant. Figure 7 further shows that the PSI reaction center protein PsaL is also lowered to about the same level as D2 (down to about 25% of that in the wild type). The same outcome pertains to the large subunit of Rubisco (RbcL). The β-subunit of the ATP-synthase (ATPβ) on the other hand was affected to a lesser extent by the loss of the CpFTSY protein in the *tla2* mutant (Fig. 7).

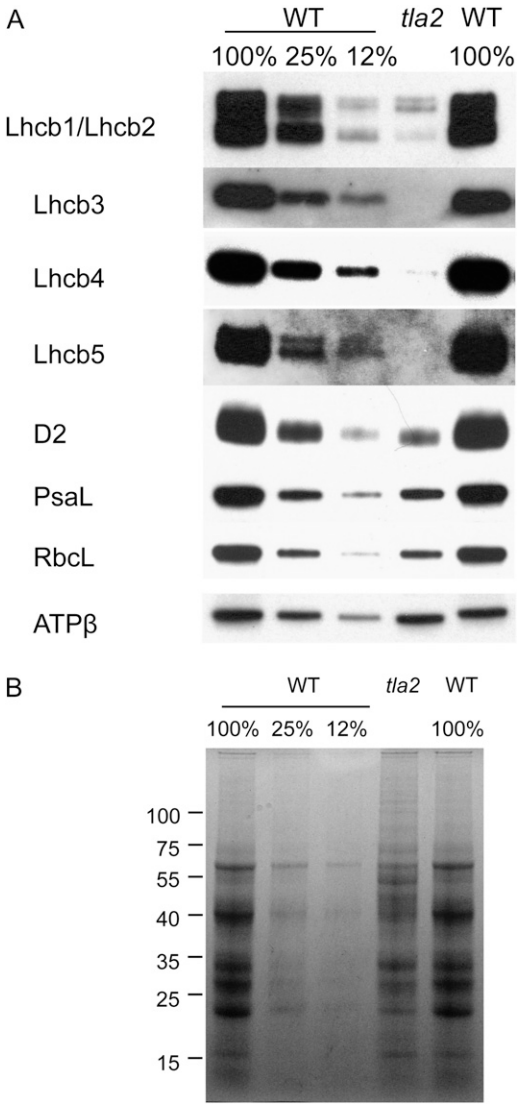

Figure 7. Western-blot analysis of the light-harvesting antenna proteins of PSII in *C. reinhardtii* wild type and the *tla2* mutant. A, Immunodetection of proteins with specific polyclonal antibodies raised against the light-harvesting proteins Lhcb1/Lhcb2, Lhcb3, Lhcb4, and Lhcb5 of Arabidopsis, the PSII reaction center protein D2, the PSI reaction center protein PsaL, Rubisco, and the β-subunit of the ATP synthase are shown. B, Coomassie-Blue-stained SDS-PAGE analysis of the samples shown in A.

To test the level of CpFTSY protein expression in the wild type and *tla2* complemented lines, western-blot analyses were conducted with specific polyclonal antibodies, directed against the recombinant CpFTSY protein of *C. reinhardtii*. No cross-reaction between antibodies and a protein band at around 39 kD could be detected in the *tla2* cell extracts, proving that *tla2* is a knockout mutant of CpFTSY (Fig. 8A). In the C4 complement, levels of the CpFTSY protein content were below 10% of those in the wild type, while C3 and C2 contained about 25% and 50% of the wild-type CpFTSY protein, respectively. The C1 complemented line was found to substantially overexpress the CpFTSY protein, as evident by the sizable dark band, seen even after a short film exposure in Figure 8A. It was estimated that cells of the C1 complemented line accumulate >5-fold CpFTSY protein than the wild type. However, this overexpression of the CpFTSY protein in the C1 complemented line did not increase the pigmentation of the cells in this strain, nor did it lower the Chl *a*/*b* ratio to a value less than that of the wild type. This finding suggests that wild-type levels of the CpFTSY protein are sufficient to meet all needs of the *C. reinhardtii* chloroplast and that levels of the CpFTSY protein in the wild type are not the limiting step in either the accumulation of Chl/cell or enhancement of the photosystem Chl antenna size.

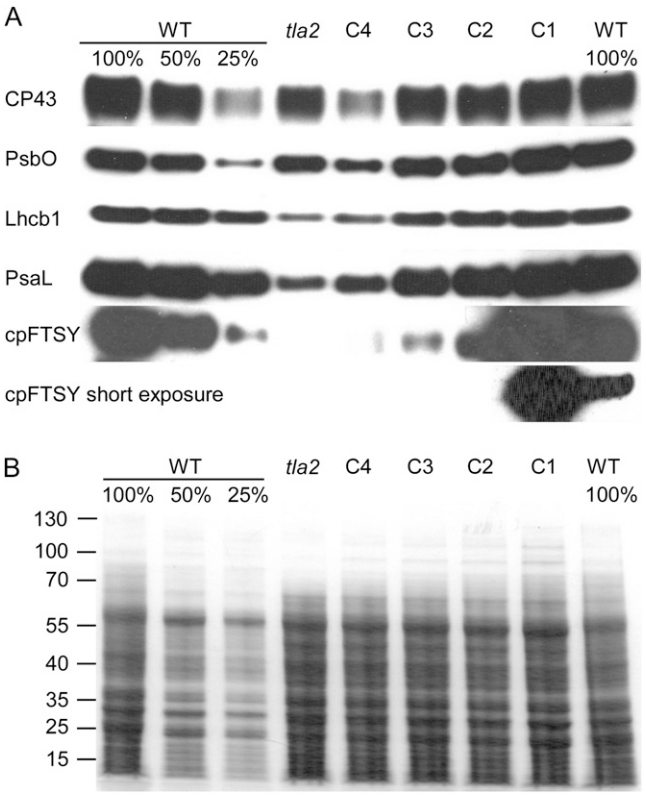

Figure 8. Western-blot analysis of *C. reinhardtii* total cell protein extracts isolated from wild type, the *tla2* mutant strain, and *tla2* lines C1, C2, C3, and C4 complemented with a wild-type copy of the *CrCpFTSY* gene. A, Immunodetection of CrCpFTSY and other thylakoid membrane proteins was performed with polyclonal antibodies against PSII subunits CP43 and PsbO, PSI subunit PsaL, and against the LHCII subunit Lhcb1 of Arabidopsis. Loading of lanes was based on Chl and corrected for the Chl content per cell so as to load proteins on an equal cells basis. B, Coomassie-Blue-stained SDS-PAGE analysis of the samples shown in A.

Intermediate between wild-type and *tla2* values of the Chl/cell and the Chl *a*/*b* ratio were observed in the C2 to C4 complemented strains. These intermediate values correlated with the level of expression of the CpFTSY protein in these complemented lines. Accordingly, levels of expression for the CpFTSY protein, the Chl/cell, and the reciprocal of the Chl *a*/*b* ratio were in the order C1 > C2 > C3 > C4 (see Fig. 8A; Table I).

Under low-light heterotrophic growth, the PSII reaction center proteins CP43 and PsbO accumulated in the *tla2* mutant to about 50% of the wild-type level, while the major PSII Chl *a*-*b* light-harvesting antenna protein Lhcb1 was lowered to a mere 10% of the wild type (Fig. 8A). The latter is consistent with the low pigmentation and also with the high Chl *a*/*b* ratio of the *tla2* mutant. The PSI reaction center protein PsaL was also found to be lower in abundance, down to about 10% in the *tla2* mutant relative to the wild type. The different relative abundance of PSI and PSII in the *tla2* mutant compared to the wild type under heterotrophic, low-light growth versus photoautotrophic, medium-light growth can be explained as a consequence of the changed light and growth conditions that prevail, rather than to a direct consequence of the *tla2* mutation. The level of these proteins was restored in the C1 complemented line, while the other complemented lines showed intermediate protein contents directly correlating with the CpFTSY expression in these strains.

CpFTSY Is Localized in the Chloroplast Stroma

Two protein-targeting servers, namely TargetP and ChloroP, predicted chloroplast targeting of the precursor CpFTSY protein. The analysis with TargetP included a reliability score, which was rather low in the case of the CpFTSY apoprotein, indicating a weak prediction. However, both programs predicted that the first 36 amino acids probably act as the chloroplast transit peptide. To investigate if the CpFTSY protein is indeed chloroplast localized, an intact chloroplast-enriched fraction was isolated from *C. reinhardtii* and probed by western-blot analysis (Fig. 9). Included in this analysis were proteins from total cell extract, thylakoid membrane fraction, soluble fraction of whole cells, and intact chloroplasts. For the total cell extract and the chloroplast-enriched fraction, equal amounts of Chl were loaded. The western-blot analysis results showed that the amount of the CpFTSY protein was about the same in total cell and chloroplast extracts (Fig. 9A). No CpFTSY antibody cross-reaction could be detected in the membrane fraction, whereas a strong CpFTSY cross-reaction was noted

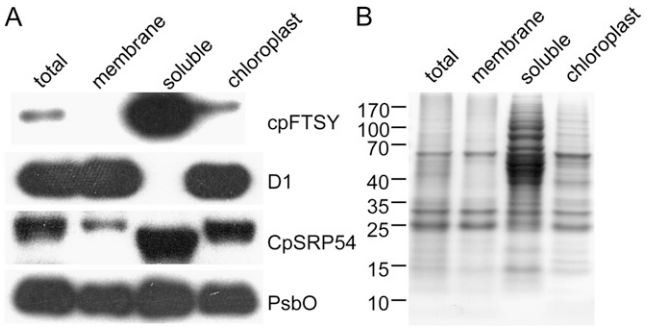

Figure 9. Cell fractionation and localization of the CpFTSY protein. A, Immunoblot analysis of wild-type total cell protein extract (1.5 μg Chl loaded), total membrane extract (1.5 μg Chl loaded), total soluble fraction (75 μg of protein loaded), and isolated chloroplast extract (1.5 μg Chl loaded). Western-blot analysis was conducted with specific polyclonal antibodies raised against the CrCpFTSY, CrCpSRP54, PsbO, or D2 proteins. B, Coomassie-Blue-stained SDS-PAGE analysis of the samples shown in A.

with proteins in the soluble extracts of *C. reinhardtii*. These results are consistent with predictions made on the basis of bioinformatic analysis (DAS, HMMTOP, PredictProtein, SOSUI, TMHMM, TMpred, and TopPred software) assigning soluble properties to the CpFTSY protein. A similar profile was noted in western blots of the above-mentioned protein extracts, probed with specific polyclonal antibodies raised against the CpSRP54 protein of *C. reinhardtii* (Fig. 9A). The latter is postulated to function in tandem with the CpFTSY protein (see "Discussion" section). Figure 9A also shows western-blot analysis results of the above-mentioned protein extracts with specific polyclonal antibodies raised against the D1 and PsbO proteins of PSII, the latter serving as controls for the purity of the fractions that were employed in the localization of the CpFTSY protein.

Chl-Protein Analysis of Wild-Type and *tla2* Mutant by Nondenaturing Deriphat-PAGE

The pale-green phenotype of the *tla2* mutant, its low Chl content per cell, the higher than wild type Chl *a*/*b* ratio, and the lower content of thylakoid membrane proteins (PSII-RC, Lhcb1, PSI-RC) all indicate alterations in the organization of the photosynthetic apparatus and in the light-harvesting antenna of this strain. Further characterization of these changes was afforded by nondenaturing Deriphat-PAGE analysis. In photosynthetic organisms the photosystems are organized in large complexes (holocomplexes) with the photosystem core and LHC tightly coupled and integral to the thylakoid membrane. However, the subcomplexes can be separated by nondenaturing Deriphat-PAGE (Peter and Thornber, 1991). We used this method with thylakoid membrane preparations from *tla2*, its complemented C1 to C4 lines, and a wild-type control. Four different pigment-containing protein complexes could be distinguished in the PAGE analysis of the wild type: large complexes, migrating to about 660 kD, PSI and PSII complexes, including their light-harvesting antennae, PSII dimers (approximately 500 kD), PSII monomers (approximately 250 kD), and LHC-II trimers at around 70 kD (Fig. 10A). In the *tla2* mutant most of these Chl-protein native bands were substantially reduced or absent. PSII-LHC-II supercomplexes and PSII dimers could not be detected on the green native gels. On the other hand, the intensity of the PSII monomer band did not change significantly in the *tla2* mutant relative to the wild type (lanes loaded on a per-cell basis). In the *tla2*-complemented lines the green band attributed to PSII monomers stayed at about the

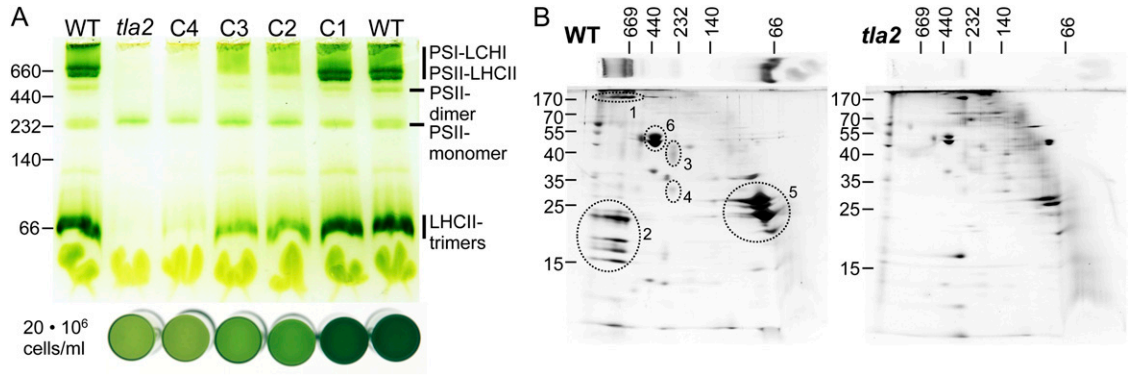

Figure 10. Analysis of photosynthetic complexes from thylakoid membranes, resolved by nondenaturing Deriphat-PAGE and denaturing second-dimension electrophoresis. Samples tested were from wild type, *tla2* mutant, and *tla2* lines C1, C2, C3, and C4 complemented with a wild-type copy of the *CrCpFTSY* gene. A, Pigment-protein complexes resolved by nondenaturing Deriphat-PAGE. Protein complexes were identified by their molecular mass of the first nondenaturing and second denaturing dimension. Masses of the marker on the left are given in kD. B, Silver-nitrate-stained second denaturing dimension from wild type and *tla2*. 1, PSI reaction center proteins PsaA and PsaB dimer; 2, LHCI proteins; 3, PSII reaction center proteins CP43 and CP47; 4, PSII reaction center proteins D1 and D2; 5, LCHII proteins; 6, α- and β-subunit of the ATP synthase. Molecular size markers are given in kD. [See online article for color version of this figure.]

same level, while all other green bands increased in their intensity in parallel with the degree of *tla2*-CpFTSY complementation.

A two-dimensional analysis of the protein complexes resolved by the native page was also undertaken (Fig. 10B). Putative proteins were identified based on their M_r in the two-dimensional SDS-PAGE. Results obtained from the two-dimensional denaturing SDS-PAGE analysis were consistent with the notion of substantial depletion of the LHC from the *tla2* mutant. The analysis further revealed that the abundance of the ATP synthase in *tla2* thylakoids was also slightly lowered by the mutation since the α- and β-subunits of this complex were not as abundant as those in the wild type (Fig. 10B).

DISCUSSION

The *C. reinhardtii tla2* locus encodes for one of the components of the CpSRP, namely the nuclear-encoded and chloroplast-localized FTSY protein. This conclusion is based on the successful complementation of the *tla2* mutant with a cDNA construct of the newly cloned *CrCpFTSY* gene. The product of the *CrCpFTSY* gene shares a sequence identity of about 46% with the CpFTSY protein of Arabidopsis and maize, while the sequence identity of CpFTSY of these two plant species to each other is even greater, at 74%. This is not surprising considering the evolutionary distance between higher plants and green algae, but can explain differences in the plant versus algal phenotype of CpFTSY-deletion mutants. Earlier work in higher plants, i.e. pea (*Pisum sativum*; Tu et al., 1999), maize (Asakura et al., 2004), and Arabidopsis (Asakura et al., 2008) indicated that CpFTSY is either associated with the thylakoid membrane or equally partitioned between the soluble stroma and thylakoid membrane in the chloroplasts. However, the CrCpFTSY in this study was localized exclusively in the soluble chloroplast stroma fraction of *C. reinhardtii*. This discrepancy could be explained in part by slightly different properties of the plant versus algal CpFTSY, as evidenced by their amino acid sequence divergence. Another source of the discrepancy could be traced to differences in cell fractionation and thylakoid membrane isolation protocols between plants and unicellular green algae. In the latter, powerful sonication or French-press methods are employed to rupture the cell wall, an approach that invariably breaks the continuity of the thylakoid membrane in the chloroplast. Under these harsh mechanical fractionation conditions, it is possible that loosely bound CpFTSY proteins separate from the nascent thylakoid membranes.

Role of CpFTSY in LHC Assembly

It has been reported that CpFTSY of higher plants is essential for the biogenesis of thylakoid membranes, including both the assembly of the Chl *a-b* LHCs and that of the two photosystems (Asakura et al., 2008). CpFTSY is assumed to play a role in the correct integration of these transmembrane complexes in developing thylakoid membranes. Accordingly, *cpftsy* null mutants of higher plants could not grow photoautotrophically, as they lacked not only the LHC but also PSII and PSI. The deletion mutant of *cpftsy* in *Chlamydomonas*, as evidenced in this work, showed a significantly different phenotype: Most of the peripheral light-harvesting antenna complexes of PSI and PSII did not accumulate in the thylakoid membrane. However, and contrary to the observation of seedling-lethal *cpftsy* mutants in higher plants, the *tla2* mutant of *C. reinhardtii* grew well photoautotrophically with a quantum yield of photosynthesis similar to that of the wild type. This substantially different property of the *CrCpFtsY* gene in green microalgae will permit application of the *CrCpFtsY* gene in the generation of green microalgal strains with a TLA phenotype, useful in commercial applications comprising biomass, biofuels, and industrial chemicals production.

The CpFTSY in green microalgae plays a role in the integration of the photosystem-peripheral LHCs into the thylakoid membrane. It presumably functions together with the other SRP pathway proteins CpSRP54, CpSRP43, and ALB3 (Fig. 11). CpSRP43 was shown to be a specific chaperon for light-harvesting proteins and is needed to prevent and dissolve aggregation of the hydrophobic domains of the light-harvesting proteins after import into the chloroplast (Falk and Sinning, 2010; Jaru-Ampornpan et al., 2010). CpSRP54 and CpFTSY are thought to bind to this LHC-protein/CpSRP43 complex and guide it to the membrane-bound translocase ALB3. We suggest that the ALB3 translocase is specifically localized in the polar regions of the chloroplast, where the thylakoid biogenesis takes place. There, it receives the LHC-CpSRP43-CpSRP54-CpFTSY complex and guides the LHC in the nascent thylakoid membrane lipid bilayer. This concept of the localization of the LHC assembly apparatus is opposite to the notion of a uniform distribution of the ALB3 translocase throughout the entire thylakoid membrane. Upon GTP hydrolysis, the LHC protein is integrated into the thylakoid membrane (Tu et al., 1999). SRP proteins CpSRP54 and ALB3 are needed for the proper integration of other transmembrane proteins, as evident by the phenotype generated in the corresponding knockout mutants (Amin et al., 1999; Bellafiore et al., 2002).

We conclude that there is a dichotomy in the function of the CpFTSY protein between green microalgae (e.g. *C. reinhardtii*) and higher plants (e.g. Arabidopsis and maize), where absence of the CpFTSY in *C. reinhardtii* impacts the assembly of the LHC-II only, versus the evidence in higher plants, where absence of the CpFTSY impacts the assembly of the entire photosystems (Asakura et al., 2004, 2008). This is clearly supported by the fact that the *tla2* mutants grow well photo autotrophically and have functional PSII and PSI reaction centers. The lower reaction center protein

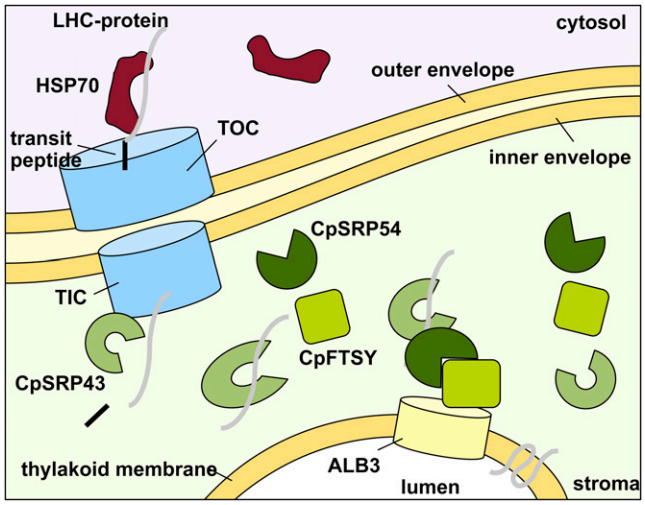

Figure 11. Working model of the function of the CrCpSRP transmembrane complex assembly system in the model green algae *C. reinhardtii*. Precursor LHC proteins are targeted to the chloroplast via the transit peptide and the heat shock protein HSP70, which functions as a molecular chaperon to prevent aggregation of the preassembled proteins. Chloroplast protein import is facilitated by the envelope-localized TOC and TIC complexes, which catalyze protein import through the outer and inner envelope membranes of the chloroplast. The transit peptide is cleaved off and the molecular chaperon CpSRP43 binds to the incoming light-harvesting protein to prevent its aberrant misfolding and aggregation. CpSRP54 and CpFTSY guide this CpSRP43-LHC complex to the membrane-bound translocase ALB3. Upon integration of the light-harvesting protein into the nascent thylakoid membrane, the LHC-CpSRP43-CpSRP54-CpFTSY complex disassembles, making the SRP subunits available for another carry-and-assembly cycle. [See online article for color version of this figure.]

content of the *tla2* strain compared to a wild type is an indication of overall lower thylakoid membrane abundance in the chloroplast of the mutant. Inability to assemble the imported light-harvesting proteins in the *tla2* mutant may trigger a feedback inhibition in Chl biosynthesis, indirectly affecting the Chl supply and lowering the chloroplast ability to assemble the full amount of PSII and PSI reaction centers. In spite of the total absence of the CpFTSY, the *tla2* mutant retained assembly activity for some of the light-harvesting proteins. It has been reported that chaperon CpSRP43 alone is sufficient to form a complex with the translocase ALB3 (Bals et al., 2010) and this could suffice to explain the observation that some light-harvesting antenna proteins can still become incorporated into the thylakoid membrane, albeit with a much lower efficiency.

It is of interest that rates of cellular respiration in the *tla2* mutant were substantially lower, down to about 30% of those measured in the wild type. A truncated Chl antenna in the photosynthetic apparatus should not a priori affect the cell's respiration capacity (Polle et al., 2000, 2003). Rather, loss of respiration fitness in the *tla2* mutant, and possibly also loss of PSII and PSI content, could be attributed to the loss of a number of genes flanking the pJD67 insertion site, which were deleted or rearranged in the *tla2* genomic DNA. The deleted genes and the 358-kb genomic DNA 180° flip are proximal to the insertion site and, therefore, could not be recovered in spite of the many crosses of the original *tla2* strain with a wild-type counterpart. The deleted genes, and those contained in the 358-kb 180° flip, are predicted open reading frames of unknown function, and were not further analyzed in this work. Accordingly, the possibility could not be excluded that one of these deleted or rearranged genes in the *tla2* mutant adversely affected properties of respiration, PSII and PSI content, and/or cell size.

CpFTSY, a Tool for the Regulation of the Chl Antenna Size Specifically in Microalgae

There is current interest and on-going efforts to renewably generate fuel and chemical products for human consumption, through the process of microalgal photosynthesis. Such bioproducts include H_2 and other suitable biofuel molecules (Melis, 2007; Hankamer et al., 2007; Hu et al., 2008; Greenwell et al., 2010; Mata et al., 2010), antigens (Dauvillée et al., 2010, Michelet et al., 2011), and high-value bioproducts (Mayfield et al., 2007). Sunlight energy conversion in photosynthesis must take place with the utmost efficiency, as this would help to make renewable fuel and chemical processes economically feasible. In plants and algae, the solar energy conversion efficiency of photosynthesis is thus a most critical factor for the economic viability of renewable fuel and chemical production (Melis, 2009). It has been shown that high-density cultures of algae with a truncated Chl antenna size are photosynthetically more productive under bright sunlight, due to the elimination of overabsorption and wasteful dissipation of excess energy (Nakajima and Ueda, 1997, 1999; Melis et al., 1999; Polle et al., 2003; Melis, 2009). The *tla2* mutant has a permanently truncated light-harvesting antenna size phenotype and, in spite of a few collateral mutations in the plasmid insertion region, it shows a higher per-Chl photosynthetic productivity than the wild-type cells. The DNA insertional mutagenesis is thus preferred over random chemical or UV-induced mutagenesis, where dozens, if not hundreds of mutations adversely impact cell fitness and productivity (Huesemann et al., 2009).

The smaller light-harvesting Chl antenna size in the *tla2* mutant requires a higher intensity to saturate photosynthesis than that in the wild type (Fig. 2). Thus, under limiting irradiance conditions in the wild, individual *tla2* cells would be at a disadvantage over their wild-type counterparts, as their light-harvesting ability has been compromised. It follows that the *tla2* mutant strain, if released in the environment, would not be able to compete with fully pigmented strains and thus cannot survive. In high-density cultures, however, at light intensities greater than 800 μmol photons m^{-2} s^{-1}, the *tla2* mutant strains would collec-

tively show greater productivity than their wild-type counterparts, due to elimination of overabsorption and wasteful dissipation of sunlight by the former. Accordingly, application of the CpFTSY gene in *tla2* type of mutations in microalgae can serve to minimize the ability of individual cells to overabsorb sunlight but at the same time helping to substantially improve the productivity of the overall mass culture.

MATERIALS AND METHODS

Cell Cultivation

Chlamydomonas reinhardtii strains CC-503 cw92 mt+, CC-425 arg2 cw15 sr-u-2-60 mt+, CC-125 wild-type mt+ 137C, obtained from the *Chlamydomonas* Center (http://www.chlamy.org/), and laboratory strains 4A+ and *tla2* were maintained under orbital shaking in 100-mL liquid cultures in Erlenmeyer flasks at 25°C under continuous illumination at low light (30 μmol photons m^{-2} s^{-1}). Irradiance was provided by balanced cool-white and warm-white fluorescent lamps. Cells were grown photoheterotrophically in TAP medium (Gorman and Levine, 1965), or photoautotrophically in high-salt (HS) medium (Harris, 1989) under a combination of cool-white, warm-white fluorescent, and incandescent irradiance at a light intensity of 450 μmol photons m^{-2} s^{-1}. For physiological measurements, cultures were harvested during the logarithmic growth phase (approximately 1–3 $\times$ 10^6 cells/mL).

Cell Count and Chl Determination

Cell density was measured using an improved Neubauer ultraplane hemacytometer and a BH-2 light microscope (Olympus). Pigments from intact cells or thylakoid membranes were extracted in 80% acetone and cell debris removed by centrifugation at 20,000*g* for 5 min. The absorbance of the supernatant was measured with a Shimadzu UV-1800 spectrophotometer, and the Chl concentration of the samples was determined according to Arnon (1949), with equations corrected as in Melis et al. (1987).

Mutagenesis and Screening Protocols

Mutants of *C. reinhardtii* were obtained upon DNA insertional mutagenesis and transformation with plasmid DNA by the glass-bead method, as described in Debuchy et al. (1989). Parental strain CC-425, an arginine auxotroph, was transformed with 1 μg *Hin*dIII linearized plasmid pJD67, containing the structural gene (*ARG7*) of the argininosuccinate lyase to complement the Arg-requiring phenotype of the CC-425 strain (Davies et al., 1994, 1996). Wild-type strain CC-503 was transformed with 0.5 μg of *Kpn*I linearized pBC1 plasmid (a gift from the lab of Dr. Kris Niyogi) conferring paromomycin resistance. Transformants were selected on TAP-only media and initially screened upon measurement of the Chl *a*/*b* ratio of the strains, following extraction of Chl with 80% acetone. A Biotek Epoch spectrophotometer equipped with a 96-well plate reader was used in these measurements.

Nucleic Acid Extractions

C. reinhardtii genomic DNA was isolated for PCR analysis using Qiagen's plant DNA purification kit. For Southern-blot analysis, genomic DNA was isolated by harvesting cells from a 50-mL aliquot of the culture upon centrifugation at 5,000*g* for 5 min, followed by resuspension of the pellet in 500 μL sterile water. Cells were lysed upon addition of 500 μL lysis buffer containing 2% SDS, 400 mM NaCl, 40 mM EDTA, 100 mM Tris/HCl (pH 8.0), and upon incubation for 2 h at 65°C. To this mix, 170 μL of 5 M NaCl solution was added. SDS and carbohydrates where precipitated upon addition of 135 μL 10% cetyltrimethylammonium bromide (CTAB) in 0.7 M NaCl and incubation for 10 min at 65°C. They were extracted by mixing with chloroform: isoamylalcohol 24:1 followed by centrifugation at 20,000*g* for 5 min. Proteins were removed by extraction with phenol:chloroform:isoamylalcohol 25:24:1 solution. RNA in the water phase was digested using 10 ng/mL RNase A and upon incubation at 37°C for 20 min. RNase A was removed by extraction with phenol:chloroform:isoamylalcohol 25:24:1 solution. Desalting of the DNA solution was achieved upon precipitation with isopropanol and resuspension in 10 mM Tris/HCl (pH 8.0).

Southern-Blot Analysis

Approximately 5 μg genomic DNA was digested by various restriction enzymes (New England Biolabs, Inc.) in a 500-μL volume at 37°C with overnight incubation (16 h). The digested DNA was precipitated with isopropanol, washed in 70% ethanol, and resuspended in 20 μL buffer containing 5 mM Tris/HCl pH 8.0. DNA fragments were separated on a 0.6% agarose gel, transferred on a positively charged nylon membrane (Hybond-N^+; Amersham), and UV cross-linked. Probes were obtained upon PCR reactions using specific primers (Supplemental Table S1) and the pJD67 plasmid as template DNA, and labeled with alkaline phosphatase using the gene images AlkPhos direct labeling and detection system kit (Amersham). The manufacturer's protocol was used for labeling, hybridization, washing, and signal detection with the following modifications: hybridization temperature and primary washing buffer temperature was maintained at 72°C.

Genetic Crosses and Analyses

All genetic crosses and strain matings were performed according to the protocol of Harris (1989). Prior to any physiological analysis, putative *tla* mutants were crossed four times to a laboratory-generated *Chlamydomonas* strain 4A+ (*arg2*). For cosegregation analysis of the *tla2* phenotype with the pJD67 insert, *tla2* was crossed to AG1x3.24 (ARG7-8$^-$). Progeny were plated on TAP medium containing Arg (TAP + Arg) and also on regular TAP-only medium (−Arg). Moreover, PCR reactions were used to test for cosegregation of the *tla2* phenotype with the pJD67 insert, using the HK128/HK126 (Supplemental Table S1) insertion-flanking sequence-specific primers set and a DNA isolation control HK135/HK134 (Supplemental Table S1).

Measurements of Photosynthetic Activity

The oxygen evolution activity of the cultures was measured at 22°C with a Clark-type oxygen electrode illuminated with light from a halogen lamp projector. A Corning 3-69 filter (510-nm cutoff filter) defined the yellow actinic excitation via which photosynthesis measurements were made. Samples of 5-mL cell suspension containing 1.3-μM Chl were loaded into the oxygen electrode chamber. Sodium bicarbonate (100 μL of 0.5 M solution, pH 7.4) was added to the cell suspension prior to the oxygen evolution measurements to ensure that oxygen evolution was not limited by the carbon supply available to the cells. After registration of the rate of dark respiration by the cells, samples were illuminated with gradually increasing light intensities. The rate of oxygen exchange (uptake or evolution) under each of these irradiance conditions was recorded continuously for a period of about 5 min.

Isolation of Thylakoid Membranes

Cells were harvested by centrifugation at 1,000*g* for 3 min at 4°C, the pellet was stored frozen at −80°C until all samples were ready for processing. Samples were thawed on ice and resuspended with ice-cold sonication buffer containing 50 mM Tricine (pH 7.8), 10 mM NaCl, 5 mM $MgCl_2$, 0.2% polyvinylpyrrolidone 40, 0.2% sodium ascorbate, 1 mM aminocaproic acid, 1 mM aminobenzamidine, and 100 μM phenylmethylsulfonyl fluoride (PMSF). Cells were broken by sonication in a Branson 250 cell disrupter operated at 4°C, three times for 30 s each time (pulse mode, 50% duty cycle, output power 5) with 30-s cooling intervals on ice. Unbroken cells and starch grains were removed by centrifugation at 3,000*g* for 4 min at 4°C. Thylakoid membranes were collected by centrifugation of the first supernatant at 75,000*g* for 30 min at 4°C. The thylakoid membrane pellet was resuspended in a buffer containing 50 mM Tricine (pH 7.8), 10 mM NaCl, 5 mM $MgCl_2$ for spectrophotometric measurements, or 250 mM Tris/HCl (pH 6.8), 20% glycerol, 7% SDS, and 2-M urea for protein analysis.

Spectrophotometric and Kinetic Analyses

The concentration of the photosystems in thylakoid membranes was measured spectrophotometrically from the amplitude of the light-minus-dark absorbance difference signal at 700 nm (P700) for PSI, and 320 nm (Q_A) for PSII (Melis and Brown, 1980; Melis, 1989; Smith et al., 1990). The functional light-

harvesting Chl antenna size of PSI and PSII was measured from the kinetics of P700 photooxidation and Q_A photoreduction, respectively (Melis, 1989).

5′ and 3′ RACE Analysis

Total RNA was isolated from CC-503 cells in the early log phase of growth (0.5×10^6 cells mL^{-1}) using the Trizol reagent (Invitrogen). Genomic DNA in these samples was digested according to the protocol provided by the Turbo DNA-free kit (Ambion). The RNA sample was used immediately for the 5′ and 3′ RACE analysis using the FirstChoice RLM-RACE kit (Ambion) and with suitable primers (HK297/HK298 outer/inner for 3′ RACE; HK289/HK290 outer/inner for 5′ RACE; Supplemental Table S1). The manufacturer's protocol was followed in all procedures.

Transformation of *C. reinhardtii*

Complementation of the *tla2* strain was achieved by cotransformation of the mutant with BAC clones 08N24 and 36L15 and pBC1 plasmid (conferring paromomycin resistance) using the highly efficient electroporation method (Shimogawara et al., 1998). pBC1 contains a paromomycin resistance gene (selectable marker) operated under the control of the *C. reinhardtii Hsp70A* and *RbcS2* promoters (Sizova et al., 2001). Further, *CpFTSY* cDNA was cloned into pSL18 and incorporated into the genomic DNA of the *tla2* mutant using the conventional glass bead transformation protocol (Kindle, 1990). pSL18 also contains a paromomycin resistance gene (selectable marker) operated under the control of the *C. reinhardtii Hsp70A* and *RbcS2* promoters (Sizova et al., 2001) and linked to the PsaD promoter and terminator that was used to express the *CpFTSY* gene. Transformants were isolated upon screening independent cell lines on the basis of the measured Chl *a*/*b* ratio of the cells.

H6-CpFTSY and H6-CpSRP54 Recombinant Protein Expression and Purification

Standard procedures were employed for isolation of plasmid DNA, restriction analysis, PCR amplification, ligation, and transformation (Sambrook et al., 1989). Plasmid DNA was prepared with a plasmid purification kit supplied by Qiagen. Restriction enzymes were purchased from New England Biolabs. They were used according to the recommendation of the vendors. Oligonucleotides were purchased from Bioneer and sequence details are given in Supplemental Table S1.

Escherichia coli Rosetta (DE3) cells were transformed with plasmid pET28-H_6*FtsY* and pET28-H_6-*SRP54* and grown in 1 L of Luria-Bertani medium in 2-L Fernbach flasks on a rotary shaker at 37°C to a density of about $OD_{600} = 0.8$. Protein expression was induced by the addition of 0.2-mM isopropyl β-D-thiogalacto-pyranoside, and growth was continued for 4 h at 37°C. Cells were harvested by centrifugation at 4,500*g* for 10 min at 4°C. Cells were resuspended in 10 mL of buffer I (50 mM Tris/HCl, pH 8.0, 400 mM NaCl, 10 mM beta-mercaptoethanol and lysed in a French pressure cell operated at 1,000 ψ. To remove cell debris, the cell lysate was centrifuged at 13,000*g* for 10 min at 4°C. The supernatant was mixed with 4 mL of Ni^{2+}-NTA agarose resin (Qiagen), equilibrated with buffer I, and incubated for 1 h at 4°C. The slurry was poured into a column, the flow through was discarded, and the slurry washed at 4°C with buffer I^5 (buffer I supplemented with 5 mM imidazole) and buffer I^{25} (buffer I supplemented with 25 mM imidazole). H_6-FtsY was eluted with buffer I^{200} (buffer I supplemented with 200 mM imidazole). Protein fractions were analyzed by SDS-PAGE and fractions containing H_6-FtsY were pooled. The purified protein was concentrated with Amicon Ultra 15, 30-kD cutoff devices (Millipore) to a final volume of 3 mL (2–3 mg/mL). The concentrate was centrifuged at 15,000*g* for 5 min to remove precipitated protein. The resulting proteins were pure as judged by SDS-PAGE analysis and migrated to the expected molecular mass of about 39 kD for the CpFTSY and 54 kD for the CpSRP54 proteins, respectively (results not shown). Specific polyclonal antibodies were generated in rabbit against the recombinant purified H6-CpFtsY and H6-CpSRP54 protein (ProSci Incorporated).

Analysis of Genomic DNA Flanking the Plasmid Insert Site

C. reinhardtii genomic DNA flanking the plasmid insertion site was amplified using a TAIL-PCR protocol (Liu et al., 1995), optimized for *Chlamydomonas* genomic DNA, as recently described (Chen et al., 2003; Dent et al., 2005). Primers used for the TAIL-PCR are listed in Supplemental Table S1. Briefly, flanking genomic DNA was amplified by PCR from the region adjacent to the inserted pJD67 plasmid that was used for DNA insertional mutagenesis. Specific primers for primary, secondary, and tertiary reactions were designed (Supplemental Table S1). Two arbitrary degenerate primers were tested for amplification, HK030 and HK031, as previously described (Dent et al., 2005). The general TAIL-PCR protocol of Liu et al. (1995) was used with minor modifications for the various PCR amplification reactions. Nucleotide sequences of the resulting PCR products were obtained via an ABI3100 sequence analyzer. *Chlamydomonas* genomic DNA sequence information was obtained from the *Chlamydomonas* Genome Project Web site (http://genome.jgi-psf.org/Chlre4/Chlre4.home.html and/or http://www.phytozome.net/chlamy/).

C. reinhardtii Cell Fractionation

C. reinhardtii strain CC-503 (cw92 mt+) was cultured photoheterotrophically in TAP medium (Harris, 1989) upon illumination of 30 μmol photons m^{-2} s^{-1} at 25°C. Cultures were grown to the early logarithmic phase with a maximum optical density of $OD_{750} = 0.5$ (approximately 6×10^6 cells mL^{-1}) in 250-mL Erlenmeyer flasks and harvested by centrifugation at 1,500*g* for 5 min in a swinging bucket rotor (Eppendorf 5810 R centrifuge) prior to cell fractionation approaches. Cells were resuspended in cell lysis buffer (20 mM HEPES-KOH pH 7.5, 5 mM $MgCl_2$, 5 mM β-mercaptoethanol, and 1 mM PMSF) at 4°C and broken in a French-press chamber (Aminco) at 600 ψ. Total supernatant and total membrane were separated by centrifugation at 17,900*g* for 30 min at 4°C. Total membranes were washed twice and resuspended to a final Chl concentration of 1 mg/mL with thylakoid membrane buffer (20 mM HEPES-KOH pH 7.5, 300 mM sorbitol, 5 mM MgCl2, 2.5 mM EDTA, 10 mM KCl, and 1 mM PMSF). Total cell pellets were resuspended to 1 mg Chl per mL with 1 volume of lysis buffer and 1 volume of 2× denaturing cell extraction buffer (0.2 M Tris, pH 6.8, 4% SDS, 2 M urea, 1 mM EDTA, and 20% glycerol). In addition, all denaturing samples were supplemented with a 5% (v/v) of β-mercaptoethanol and centrifuged at 17,900*g* for 5 min prior to gel loading. Chloroplast-enriched fractions were isolated from synchronized cultures with 12-h light/dark cycles of cell-wall-deficient strain CC-503 (cw92 mt+) as in Zerges and Rochaix (1998).

Western-Blot Analysis

Western-blot analyses were performed with protein from cell extracts, resolved in precast SDS-PAGE Any KDTM (BIO-RAD). Loading of samples was based on equal protein, quantified by colorimetric Lowry-based DC protein assay (BIO-RAD), and transferred to a polyvinylidene difluoride membrane (Immobilon-FL 0.45 μm, Millipore) via a tank transfer system. Cross-reactions with specific polyclonal antibodies raised against the Lhcb (1-5), PsbO, CP43, and PsaL from Arabidopsis (*Arabidopsis thaliana*) and CrCpFTSY, CrCpSRP54, D2, RbcL, and ATPβ from *C. reinhardtii* were visualized by Supersignal West Pico Chemiluminiscent substrate detection system (Thermo Scientific). The National Institutes of Health Image 1.62 software was employed for the deconvolution and quantification of the western-blot bands.

Nondenaturing Deriphat-PAGE

Nondenaturing Deriphat-PAGE was performed following the method developed by Peter and Thornber (1991) with the following modifications: continuous native resolving PAGE gradients (4%–15% final concentration of acrylamide) with no stacking gel were prepared. Isolated thylakoid membranes, from wild type, *tla2* mutant, and *tla2*-complemented lines C1, C2, C3, and C4 were prepared with thylakoid membrane buffer and solubilized at a Chl concentration of 2, 1, and 0.4 mg/mL, respectively, with an equal volume of surfactant 10% *n*-dodecyl-β-D-maltoside (SIGMA). Thus, a 50:1 weight ratio of surfactant to Chl was used for the wild type. Thylakoid membranes were incubated on ice for 30 min and centrifuged at 17,900*g* for 10 min to precipitate unsolubilized material. The amounts loaded per lane correspond to 10 μL of solubilized samples. Nondenaturing Deriphat-PAGE was run for 2 h in the cold room at 5 mA constant current.

One-dimensional nondenaturing Deriphat-PAGE strips were solubilized in the presence of Laemmli denaturing buffer (Laemmli, 1970) for 15

min and resolved in a denaturing 2-M urea 12% SDS-PAGE second dimension. Acrylamide gels were stained with Coomassie (Fast gelTM Blue R, GE Healthcare) or silver nitrate gel staining according to Wray et al. (1981).

Sequence data from this article can be found in the GenBank/EMBL data libraries under accession number NW_001843769.1.

Supplemental Data

The following materials are available in the online version of this article.

Supplemental Figure S1. Southern blot analysis defining copy number and integrity of inserted pJD67 plasmid into the genomic DNA of *C. reinhardtii tla2* insertional transformant.

Supplemental Figure S2. DNA insertional mutagenesis: induced reorganization of the genomic DNA in the *tla2* strain.

Supplemental Figure S3. ClustalW amino acid sequence analysis of the putative CrCpFTSY identified in this work with the cytoplasmic SRalpha subunit homolog to the FSTY.

Supplemental Table S1. Primers used in the TLA2-DeltaCpFTSY research.

Supplemental Text S1. *Chlamydomonas reinhardtii TLA2-FTSY* genomic DNA map.

ACKNOWLEDGMENTS

We thank Dr. Kris Niyogi for the AG1-3.24 (*arg2*) strain of *C. reinhardtii* and for providing the pBC1 plasmid employed in this work. We thank Dr. Jurgen Polle and Dr. Sarada Kanakagiri, as well as Dr. Thilo Ruehle, Mr. Ian McRae, and Ms. Carine Marshall, all of whom contributed to the screening of putative *tla* strains in the Melis-lab.

Received October 26, 2011; accepted November 22, 2011; published November 23, 2011.

LITERATURE CITED

Aldridge C, Cain P, Robinson C (2009) Protein transport in organelles: protein transport into and across the thylakoid membrane. FEBS J **276:** 1177–1186

Amin P, Sy DAC, Pilgrim ML, Parry DH, Nussaume L, Hoffman NE (1999) Arabidopsis mutants lacking the 43- and 54-kilodalton subunits of the chloroplast signal recognition particle have distinct phenotypes. Plant Physiol **121:** 61–70

Arnon DI (1949) Copper enzymes in isolated chloroplasts: polyphenol oxidase in *Beta vulgaris*. Plant Physiol **24:** 1–15

Asakura Y, Hirohashi T, Kikuchi S, Belcher S, Osborne E, Yano S, Terashima I, Barkan A, Nakai M (2004) Maize mutants lacking chloroplast FtsY exhibit pleiotropic defects in the biogenesis of thylakoid membranes. Plant Cell **16:** 201–214

Asakura Y, Kikuchi S, Nakai M (2008) Non-identical contributions of two membrane-bound cpSRP components, cpFtsY and Alb3, to thylakoid biogenesis. Plant J **56:** 1007–1017

Ballottari M, Dall'Osto L, Morosinotto T, Bassi R (2007) Contrasting behavior of higher plant photosystem I and II antenna systems during acclimation. J Biol Chem **282:** 8947–8958

Bals T, Dünschede B, Funke S, Schünemann D (2010) Interplay between the cpSRP pathway components, the substrate LHCP and the translocase Alb3: an *in vivo* and *in vitro* study. FEBS Lett **584:** 4138–4144

Bellafiore S, Ferris P, Naver H, Göhre V, Rochaix JD (2002) Loss of Albino3 leads to the specific depletion of the light-harvesting system. Plant Cell **14:** 2303–2314

Chen HC, Yokthongwattana K, Newton AJ, Melis A (2003) *SulP*, a nuclear gene encoding a putative chloroplast-targeted sulfate permease in *Chlamydomonas reinhardtii*. Planta **218:** 98–106

Dauvillée D, Delhaye S, Gruyer S, Slomianny C, Moretz SE, d'Hulst C, Long CA, Ball SG, Tomavo S (2010) Engineering the chloroplast targeted malarial vaccine antigens in Chlamydomonas starch granules. PLoS ONE **5:** e15424

Davies JP, Yildiz F, Grossman AR (1994) Mutants of *Chlamydomonas* with aberrant responses to sulfur deprivation. Plant Cell **6:** 53–63

Davies JP, Yildiz FH, Grossman AR (1996) Sac1, a putative regulator that is critical for survival of *Chlamydomonas reinhardtii* during sulfur deprivation. EMBO J **15:** 2150–2159

Debuchy R, Purton S, Rochaix JD (1989) The argininosuccinate lyase gene of Chlamydomonas reinhardtii: an important tool for nuclear transformation and for correlating the genetic and molecular maps of the ARG7 locus. EMBO J **8:** 2803–2809

Dent RM, Haglund CM, Chin BL, Kobayashi MC, Niyogi KK (2005) Functional genomics of eukaryotic photosynthesis using insertional mutagenesis of *Chlamydomonas reinhardtii*. Plant Physiol **137:** 545–556

Falk S, Sinning I (2010) cpSRP43 is a novel chaperone specific for light-harvesting chlorophyll *a,b*-binding proteins. J Biol Chem **285:** 21655–21661

Glick RE, Melis A (1988) Minimum photosynthetic unit size in system-I and system-II of barley chloroplasts. Biochim Biophys Acta **934:** 151–155

Gorman DS, Levine RP (1965) Cytochrome f and plastocyanin: their sequence in the photosynthetic electron transport chain of Chlamydomonas reinhardi. Proc Natl Acad Sci USA **54:** 1665–1669

Greene BA, Staehelin LA, Melis A (1988) Compensatory alterations in the photochemical apparatus of a photoregulatory, chlorophyll *b*-deficient mutant of maize. Plant Physiol **87:** 365–370

Greenwell HC, Laurens LML, Shields RJ, Lovitt RW, Flynn KJ (2010) Placing microalgae on the biofuels priority list: a review of the technological challenges. J R Soc Interface **7:** 703–726

Hankamer B, Lehr F, Rupprecht J, Mussgnug JH, Posten C, Kruse O (2007) Photosynthetic biomass and H2 production by green algae: from bioengineering to bioreactor scale-up. Physiol Plant **131:** 10–21

Harris EH (1989) The *Chlamydomonas* Source Book: A Comprehensive Guide to Biology and Laboratory Use. Academic Press, San Diego, pp 1–780

Hu Q, Sommerfeld M, Jarvis E, Ghirardi M, Posewitz M, Seibert M, Darzins A (2008) Microalgal triacylglycerols as feedstocks for biofuel production: perspectives and advances. Plant J **54:** 621–639

Huesemann MH, Hausmann TS, Bartha R, Aksoy M, Weissman JC, Benemann JR (2009) Biomass productivities in wild type and pigment mutant of *Cyclotella sp.* (Diatom). Appl Biochem Biotechnol **157:** 507–526

Jaru-Ampornpan P, Shen K, Lam VQ, Ali M, Doniach S, Jia TZ, Shan SO (2010) ATP-independent reversal of a membrane protein aggregate by a chloroplast SRP subunit. Nat Struct Mol Biol **17:** 696–702

Kindle KL (1990) High-frequency nuclear transformation of *Chlamydomonas reinhardtii*. Proc Natl Acad Sci USA **87:** 1228–1232

Kirk JTO (1994) Light and Photosynthesis in Aquatic Ecosystems, Ed 2. Cambridge University Press, Cambridge, pp 1–401

Klimyuk VI, Persello-Cartieaux F, Havaux M, Contard-David P, Schuenemann D, Meiherhoff K, Gouet P, Jones JD, Hoffman NE, Nussaume L (1999) A chromodomain protein encoded by the *Arabidopsis* CAO gene is a plant-specific component of the chloroplast signal recognition particle pathway that is involved in LHCP targeting. Plant Cell **11:** 87–99

Laemmli UK (1970) Cleavage of structural proteins during the assembly of the head of bacteriophage T4. Nature **227:** 680–685

Ley AC, Mauzerall DC (1982) Absolute absorption cross sections for the photosystem II and the minimum quantum requirement for photosynthesis in *Chlorella vulgaris*. Biochim Biophys Acta **680:** 95–106

Liu YG, Mitsukawa N, Oosumi T, Whittier RF (1995) Efficient isolation and mapping of *Arabidopsis thaliana* T-DNA insert junctions by thermal asymmetric interlaced PCR. Plant J **8:** 457–463

Luirink J, Sinning I (2004) SRP-mediated protein targeting: structure and function revisited. Biochim Biophys Acta **1694:** 17–35

Mata TM, Martins AA, Caetano NS (2010) Microalgae for biodiesel production and other applications: a review. Renew Sustain Energy Rev **14:** 217–232

Mayfield SP, Manuell AL, Chen S, Wu J, Tran M, Siefker D, Muto M, Marin-Navarro J (2007) Chlamydomonas reinhardtii chloroplasts as protein factories. Curr Opin Biotechnol **18:** 126–133

Melis A (1989) Spectroscopic methods in photosynthesis: photosystem stoichiometry and chlorophyll antenna size. Philos Trans R Soc Lond, B **323:** 397–409

Melis A (1991) Dynamics of photosynthetic membrane composition and function. Biochim Biophys Acta **1058:** 87–106

Melis A (2007) Photosynthetic H2 metabolism in *Chlamydomonas reinhardtii* (unicellular green algae). Planta **226:** 1075–1086

Melis A (2009) Solar energy conversion efficiencies in photosynthesis: minimizing the chlorophyll antennae to maximize efficiency. Plant Sci **177:** 272–280

Melis A, Anderson JM (1983) Structural and functional organization of the photosystems in spinach chloroplasts: antenna size, relative electron transport capacity, and chlorophyll composition. Biochim Biophys Acta **724:** 473–484

Melis A, Brown JS (1980) Stoichiometry of system I and system II in different photosynthetic membranes. Proc Natl Acad Sci USA **77:** 4712–4716

Melis A, Neidhardt J, Benemann JR (1999) *Dunaliella salina* (Chlorophyta) with small chlorophyll antenna sizes exhibit higher photosynthetic productivities and photon use efficiencies than normally pigmented cells. J Appl Phycol **10:** 515–525

Melis A, Spangfort M, Andersson B (1987) Light-absorption and electron transport balance between photosystem-II and photosystem-I in spinach chloroplasts. Photochem Photobiol **45:** 129–136

Merchant SS, Prochnik SE, Vallon O, Harris EH, Karpowicz SJ, Witman GB, Terry A, Salamov A, Fritz-Laylin LK, Maréchal-Drouard L, et al (2007) The Chlamydomonas genome reveals the evolution of key animal and plant functions. Science **318:** 245–250

Michelet L, Lefebvre-Legendre L, Burr SE, Rochaix JD, Goldschmidt-Clermont M (2011) Enhanced chloroplast transgene expression in a nuclear mutant of Chlamydomonas. Plant Biotechnol J **9:** 565–574

Mitra M, Melis A (2010) Genetic and biochemical analysis of the TLA1 gene in *Chlamydomonas reinhardtii.* Planta **231:** 729–740

Mussgnug JH, Wobbe L, Elles I, Claus C, Hamilton M, Fink A, Kahmann U, Kapazoglou A, Mullineaux CW, Hippler M, et al (2005) NAB1 is an RNA binding protein involved in the light-regulated differential expression of the light-harvesting antenna of *Chlamydomonas reinhardtii.* Plant Cell **17:** 3409–3421

Nakajima Y, Ueda R (1997) Improvement of photosynthesis in dense microalgal suspension by reduction of light harvesting pigments. J Appl Phycol **9:** 503–510

Nakajima Y, Ueda R (1999) Improvement of microalgal photosynthetic productivity by reducing the content of light harvesting pigments. J Appl Phycol **11:** 195–201

Peter GF, Thornber JP (1991) Biochemical composition and organization of higher plant photosystem II light-harvesting pigment-proteins. J Biol Chem **266:** 16745–16754

Pilgrim ML, van Wijk KJ, Parry DH, Sy DA, Hoffman NE (1998) Expression of a dominant negative form of cpSRP54 inhibits chloroplast biogenesis in *Arabidopsis.* Plant J **13:** 177–186

Polle JE, Benemann JR, Tanaka A, Melis A (2000) Photosynthetic apparatus organization and function in the wild type and a chlorophyll b-less mutant of Chlamydomonas reinhardtii: dependence on carbon source. Planta **211:** 335–344

Polle JE, Kanakagiri SD, Melis A (2003) *tla1,* a DNA insertional transformant of the green alga *Chlamydomonas reinhardtii* with a truncated light-harvesting chlorophyll antenna size. Planta **217:** 49–59

Powles SB, Critchley C (1980) Effect of light intensity growth on photoinhibition of intact attached bean leaflets. Plant Physiol **65:** 1181–1187

Sambrook J, Fritsch EF, Maniatis T (1989) Molecular Cloning: A Laboratory Manual. Cold Spring Harbor Laboratory Press, Cold Spring Harbor, NY, pp 1.1–7.30

Shimogawara K, Fujiwara S, Grossman A, Usuda H (1998) High-efficiency transformation of *Chlamydomonas reinhardtii* by electroporation. Genetics **148:** 1821–1828

Sizova IA, Fuhrmann M, Hegemann P (2001) A Streptomyces rimosus aphVIII gene coding for a new type phosphotransferase provides stable antibiotic resistance to Chlamydomonas reinhardtii. Gene **277:** 221–229

Smith BM, Morrissey PJ, Guenther JE, Nemson JA, Harrison MA, Allen JF, Melis A (1990) Response of the photosynthetic apparatus in *Dunaliella salina* (green algae) to irradiance stress. Plant Physiol **93:** 1433–1440

Tetali SD, Mitra M, Melis A (2007) Development of the light-harvesting chlorophyll antenna in the green alga *Chlamydomonas reinhardtii* is regulated by the novel Tla1 gene. Planta **225:** 813–829

Tu CJ, Schuenemann D, Hoffman NE (1999) Chloroplast FtsY, chloroplast signal recognition particle, and GTP are required to reconstitute the soluble phase of light-harvesting chlorophyll protein transport into thylakoid membranes. J Biol Chem **274:** 27219–27224

Wray W, Boulikas T, Wray VP, Hancock R (1981) Silver staining of proteins in polyacrylamide gels. Anal Biochem **118:** 197–203

Yi L, Dalbey RE (2005) Oxa1/Alb3/YidC system for insertion of membrane proteins in mitochondria, chloroplasts and bacteria (review). Mol Membr Biol **22:** 101–111

Zerges W, Rochaix JD (1998) Low density membranes are associated with RNA-binding proteins and thylakoids in the chloroplast of *Chlamydomonas reinhardtii.* J Cell Biol **140:** 101–110

Zouni A, Witt HT, Kern J, Fromme P, Krauss N, Saenger W, Orth P (2001) Crystal structure of photosystem II from *Synechococcus elongatus* at 3.8 A resolution. Nature **409:** 739–743